

On the seismic response of steel buckling-restrained braced structures including soil-structure interaction

Antonios K. Flogeras^{1a} and George A. Papagiannopoulos^{*2}

¹Engineer Consultant, Zakinthou 34, GR-26441 Patras, Greece

²Department of Civil Engineering, University of Patras, GR-26504 Patras, Greece

(Received December 1, 2016, Revised March 7, 2017, Accepted April 19, 2017)

Abstract. This paper summarizes estimated seismic response results from three-dimensional nonlinear inelastic time-history analyses of some steel buckling-restrained braced (BRB) structures taking into account soil-structure interaction (SSI). The response results involve mean values for peak interstorey drift ratios, peak interstorey residual drift ratios and peak floor accelerations. Moreover, mean seismic demands in terms of axial force and rotation in columns, of axial and shear forces and bending moment in BRB beams and of axial displacement in BRBs are also discussed. For comparison purposes, three separate configurations of the BRBs have been considered and the aforementioned seismic response and demands results have been obtained firstly by considering SSI effects and then by neglecting them. It is concluded that SSI, when considered, may lead to larger interstorey and residual interstorey drifts than when not. These drifts did not cause failure of columns and of the BRBs. However, the BRB beam may fail due to flexure.

Keywords: buckling-restrained braces; seismic response; soil-structure interaction; three-dimensional steel structures

1. Introduction

Buckling-restrained braces (BRB) have the advantage of developing full plastic strength in both tension and compression without exhibiting strength degradation. Therefore, BRBs constitute a very attractive alternative to conventional steel braces in regions of high seismicity.

The main disadvantage of BRB frames is the lack of a restoring mechanism that inevitably leads to large permanent deformations especially under high levels of seismic motion. These large permanent deformations can be concentrated in a story mainly because BRBs have a low post-yield stiffness (Sabelli *et al.* 2003). Nevertheless, they can be appreciably reduced but cannot be eliminated either with improved connection details (Fahnestock *et al.* 2007, Richards and Miller 2014) or by using dual systems or backup moment resisting frames (e.g., Kiggins and Uang 2006, Ariyaratana and Fahnestock 2011, Richards and Miller 2014).

Several studies have indicated that buildings are no longer practically usable if the residual interstorey drift ratio (RIDR) surpasses the threshold value of 0.5%. Erochko *et al.* (2011) showed that the average peak RIDR of BRB frames varies from 0.8% to 2% under the design basis earthquake (DBE). Given that RIDR of BRB frames could exceed the value of 0.5%, post-earthquake repair costs make BRB unattractive. Similar results have been reported

by other researchers, e.g., Sahoo and Chao (2015).

The purpose of this work is to estimate the seismic response of a number of three-dimensional framed steel structures with different configurations of BRBs, taking into account soil-structure interaction (SSI) effects. The steel structures chosen are supposed to be located in the region of Ionian Islands (Western Greece), where very high seismic loads, i.e., corresponding to a peak ground acceleration (PGA) of 0.36 g, are used for earthquake resistant design purposes. Aiming to compromise theoretical knowledge with practical demands, moment connections have been considered for all beam and column members of the structures in conjunction with low-to-medium values of the behavior (strength reduction) factor.

The seismic response results obtained involve mean values for interstorey drift ratios (IDR), residual interstorey drift ratios (RIDR) and peak floor accelerations (PFA) coming out from non-linear inelastic time-history analyses using recorded accelerograms that satisfy to the maximum extent possible the requirements of EC8 (2009). Moreover, mean seismic demands in terms of axial force and rotation in columns, of axial and shear forces and bending moment in BRB beams and of axial displacement in BRBs are also discussed. For comparison purposes, both the aforementioned response and demands results are also given when SSI is neglected.

It is demonstrated that if SSI has been considered, the RIDRs are well above the value of 0.5%, rendering the steel structure practically unusable. Peak IDRs can surpass the design drift limit, whereas PFA values normalized with respect to the peak ground acceleration (PGA) reveal that BRBs may effectively limit the accelerations transmitted to structure.

The inelastic axial displacement accommodated by the

*Corresponding author, Lecturer

E-mail: gpapagia@upatras.gr

^aMSc.

E-mail: aflogeras@teemail.gr

BRB, as a result from deformations of the frame, is consistent with the approximate value of two times the design story drift mandated by seismic codes (SEAOC 2009). Taking into account buckling resistances according to EC3 (2009) nor the axial force in columns neither the axial force in BRBs surpass their design values. The BRB beam has enough axial and shear design strengths but may fail due to flexure.

2. Description of steel BRB structures

Three dimensional steel structures, used for office-residence purposes, having 4, 6 and 8 storeys (Type A) as well as a typical 2-storey industrial building (Type B) have been selected for seismic response computations.

A typical floor plan view and front views for the 4- and 6-storey structures of Type A are shown in Figs. 1-2, respectively. Each bay has a span of 6.0 m, whereas the height of each storey has been considered to be 3.0 m. The stressed black lines in Fig. 1 indicate the position of the BRB. To study the effect of different BRB configurations, the 4, 6 & 8 structures have been analyzed employing the configurations of inverted V, diagonal bracing and multistory X-bracing as shown in Fig. 3. In that figure, the middle case of diagonal bracing corresponds to a different position of the BRBs in the frames of the perimeter from that shown in Fig. 1. Moreover, the symbols used, i.e., A4a, A4b, A4c mean that the structure under study corresponds to Type A, has 4 storeys and the BRB configuration differs and may be a (inverted V), b (diagonal) or c (multistory X). Similarly one defines, A6a, A6b, A6c and A8a, A8b, A8c

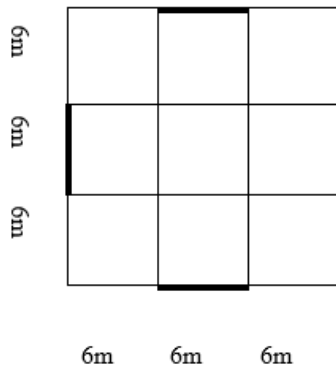


Fig. 1 Floor plan of Type A structures and location of the BRBs

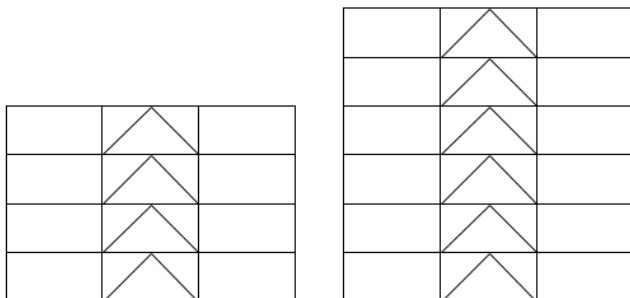


Fig. 2 Front views of 4- & 6-storey Type A structures

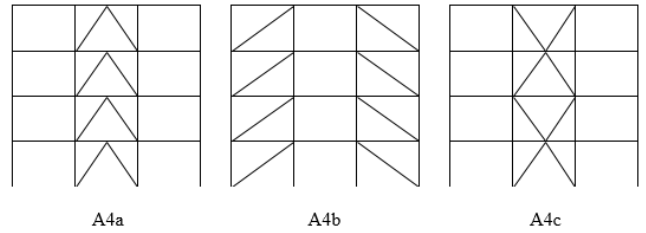


Fig. 3 Configuration of BRBs for Type A structures

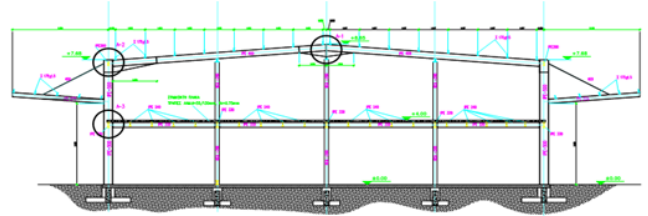


Fig. 4 Front view of Type B structure

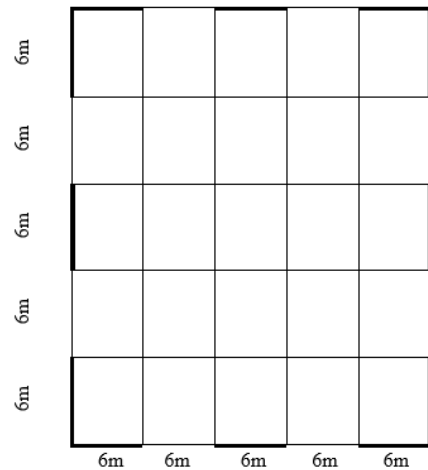


Fig. 5 Floor plan of Type B structure and location of the BRBs

for the cases of 6- and 8-storey structures of Type A, respectively.

A general view of the Type B 2-storey structure is shown in Fig. 4. Each bay has a span of 6.0 m, whereas the height of each storey has been considered to be 3.0 m. The floor plan view of Type B structure is shown in Fig. 5, where the stressed black lines indicate the position of the BRBs. Only the B2a structure has been studied which means that the inverted V configuration of Fig. 3 has been employed.

Type A & B structures have been designed according to EC3 (2009) and EC8 (2009). More specifically dead and live loads on floors have been considered to be 8.0 kN/m² and 3.0 kN/m², respectively. The design seismic load has been calculated using the design spectrum of EC8 (2009) that corresponds to a PGA of 0.36 g and to a soil of class D. Behavior factors have been considered to be equal to 2.5 for the a & c configurations and equal to 4.0 for the b configuration of Fig. 3. It should be noted that no specific values are provided in EC8 (2009) for structures having BRBs and the values selected may be enough conservative in view of the high values provided for the behavior factor

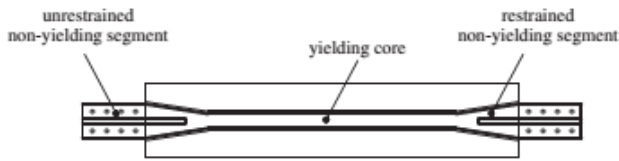


Fig. 6 Components used to calculate the equivalent area of the BRB (after Bosco and Marino 2013)

in US regulations, e.g., SEAOC (2009) and AISC (2010). Effects of accidental torsion have also been taken into account, even though, placing of BRBs on axis with the perimeter of the structures almost precludes torsional effects (Roy *et al.* 2015). Structures are initially considered to be fixed-base. SSI (due to soil of class D considered) is treated in section 4.

Standard European HEB and IPE sections (Androić *et al.* 2000) have been used for columns and beams, respectively, whereas BRBs are composed of a ductile steel core encased in a hollow section filled with concrete. The cross-sectional area of the core of the BRB is evaluated using the design storey shear (Bruneau *et al.* 2011, Bosco and Marino 2013). The elastic stiffness of BRBs is determined on the basis of an equivalent area (Bruneau *et al.* 2011, Bosco and Marino 2013). The components used to calculate the equivalent area of the BRB, i.e., the yielding core, the restrained non-yielding segment and the unrestrained non-yielding segment, are shown in Fig. 6. Steel grade S235 and a modulus of elasticity equal to 210 GPa has been used for all members.

The brace stiffness has been calculated assuming, conservatively, a yielding segment of 50% of the total length of the BRB between the work points in view of the gusset plates required. At this point, it should be noted that gusset plates have to be designed for 1.1 times the adjusted brace strength in compression and for additional forces resulting from frame action (AISC 2010, Lin *et al.* 2014). Moreover, in absence of specific criteria in EC8 (2009), the design of BRBs against non-ductile modes of failure has been performed to the extent possible according to Bruneau *et al.* (2011).

The sections for beams and columns at an exterior frame as well as the cross-sectional area of the core of each of the BRBs are shown in Table 1, where symbols, i.e., A4a etc. have been previously explained. Indicatively, the sections of beams and columns as well as the area of the core of the BRB (in m²) at an exterior frame are shown in Figs. 7 and 8 for the structures A6b and B2a, respectively. Orientation of columns follows Erochko *et al.* (2011).

The design storey drift has been considered to be 2% and the design axial displacement which the BRB should accommodate is two times this drift, i.e., 0.084 m. However, pertinent codes (EC8 2009, SEAOC 2009 and AISC 2010) do not provide any information regarding the impact of the BRB response on the seismic performance of the structure at such drift levels. Even though, cross sectional areas of the core of each BRB have been computed on the basis of the design storey shear, the distribution of BRB along the height of the structure has

been considered to be uniform in order to check the possible occurrence of large inelastic deformations on lower storeys due to SSI.

On the basis of the aforementioned design displacement, the strain hardening adjustment and compression overstrength factors, ω and β , respectively, used to define the ultimate tensile and compressive yield strengths of the BRB, have been considered in accordance to the statistical analysis of Saxey and Daniels (2014). Beams and columns have been then proportioned employing the aforementioned factors in order to remain essentially elastic using also a material overstrength factor of $1.25\omega\beta$.

All connections of steel members are considered to be moment-resisting ones, while those of the BRBs are considered to be pinned. The moment connections within the BRB frame are expected to provide reserve strength and to reduce both the drift and the residual drift of the stories.

Table 1 Design of exterior frames for Type A & B structures

Structure	Columns	Beams	Cross sectional area of the BRB core (cm ²)
A4a	HEB 320	IPE 220	52
A4b	HEB 320	IPE 220	52
A4c	HEB 320	IPE 220	52
A6a	HEB 400	IPE 240	70
A6b	HEB 400	IPE 240	70
A6c	HEB 400	IPE 240	70
A8a	HEB 500	IPE 270	87
A8b	HEB 500	IPE 270	87
A8c	HEB 500	IPE 270	87
B2a	HEB 500	IPE 270	140

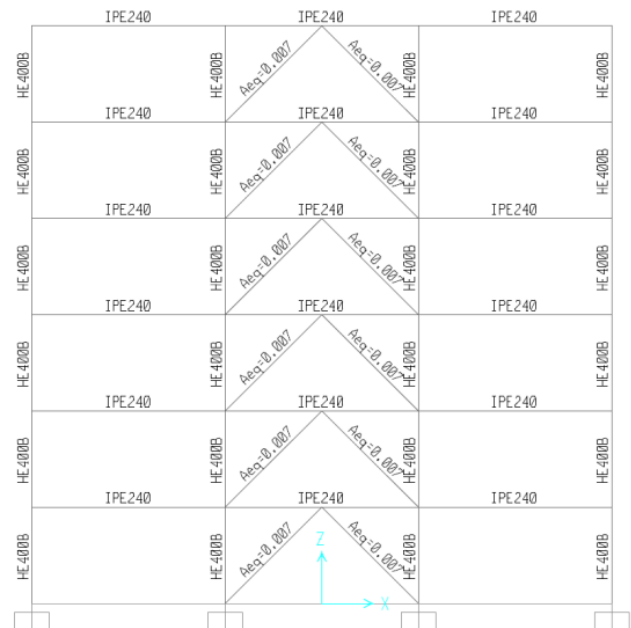


Fig. 7 Sections at an exterior frame for the A6a structure

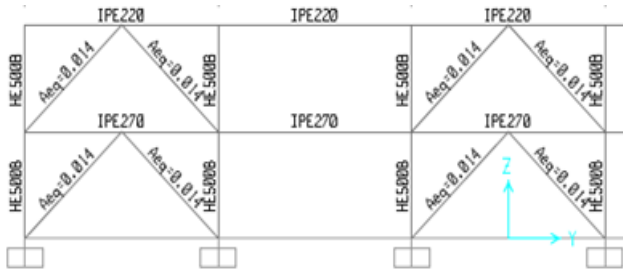


Fig. 8 Sections at an exterior frame for the B2a structure

Table 2 List of accelerograms used

Accelerogram	Earthquake	Year-Country
El Centro Array 05	Imperial Valley	1979 - U.S.A
Meloland Route Overpass	Imperial Valley	1979 - U.S.A
Parachute Test Site	Superstition Hills	1987 - U.S.A
Lucerne Valley	Landers	1992 - U.S.A
Sylmar Converter Station	Northridge	1994 - U.S.A
Takarazuka	Kobe	1995 - Japan
Lixouri	Kefalonia	2014 - Greece

3. Structural modelling & accelerograms used for non-linear inelastic analyses

The BRB structures, presented in section 2, are subjected to the 7 accelerograms of Table 2 and their seismic response is determined through non-linear inelastic dynamic time-history analyses using the computer analysis software RUAUMOKO 3D (Carr 2004). These accelerograms correspond to recordings of near-field strong ground motions because these motions have been repeatedly reported in the literature to produce large residual deformations in steel structures. Moreover, according to AISC (2010), greater deformation demands may occur for near-field strong ground motions in comparison to ordinary far-field ones. The two horizontal components of these accelerograms have been used interchangeably in both directions but their variation using an angle of incidence has not been studied.

Diaphragm action has been assumed at every floor due to the presence of a composite slab. Large deformation and second order effects have been also taken into account. Viscous damping of each structure has been considered to be 3% of critical for the first mode of vibration and for that mode for which 90% of the effective modal mass is participating. In general, assumed values for viscous damping between 0.5%-5% have no apparent impact on column demands and do not affect the results for BRBs (Richards 2009).

Beams and columns have been modelled using standard frame elements with concentrated plasticity assuming a strain hardening of 2%. The interaction of axial load with biaxial moment has been considered for all columns.

The BRB model used for seismic response purposes should include an appropriate isotropic hardening law or a combination of isotropic and kinematic hardening (Erochko *et al.* 2011, Karavasili *et al.* 2012, Zona and Dall' Asta

2012, Tsampras *et al.* 2016). This is particularly important when assessing with non-linear inelastic dynamic analysis the force demands imposed to beams and columns by the BRBs. However, for reasons of conservativeness in the seismic response calculations performed herein, the BRB has been modelled as an inelastic truss member (Carr 2004) on the basis of the equivalent area mentioned in Section 2. The post-yield stiffness of the BRB core has been assumed to be 2% of the axial elastic stiffness. A nominal yield strength of 245MPa was assumed for the BRB core in order to acknowledge the variability of yield stress in the material of the core.

Gusset plates, connecting the BRB to adjacent beams and columns have not been explicitly modelled. In view of their importance in decreasing the effectiveness of the BRB (Berman and Bruneau 2009, Wigle and Fahnestock 2010, McManus *et al.* 2013, Lin *et al.* 2014, Palmer *et al.* 2014), a detailed modelling of the gusset plates in conjunction with connection configuration has been left out for a future work. It should be stressed that by not including the gusset plates, the estimated response quantities may be significantly underestimated. The reason is that conservatively designed gusset plates may provide almost a full restraint to the beams and columns by considerably decreasing their clear flexural lengths. Nevertheless, rigid links have been assumed herein to take into account the effect of gusset plates. Inelastic column panel zone deformations have not been considered and have been also left out for a future work.

4. Soil-structure interaction

To study the influence of soil-structure interaction (SSI) in terms of seismic response results, the BRB structures are analyzed firstly by considering the effect of soil deformability then are reanalyzed as fixed-base ones. Inclusion of SSI is performed in an approximate but of enough accuracy way by employing the discrete model of Mulliken and Karabalis (1998). According to this model the foundation and its surrounding soil are effectively replaced by a spring-dashpot-mass system that acts in three dimensional space and takes into account horizontal and vertical translations, rocking and torsion. The values of the spring-dashpot-mass system are calculated on the basis of the dimensions of the footings using the formulas provided in Mulliken and Karabalis (1998). In cases of raft foundations, this discrete model can still be used. This is performed by partitioning the area of the raft foundation into smaller areas and by assigning to each one of these areas a discrete spring-dashpot-mass system.

The BRB structures have been designed, as mentioned in section 2, for a soil of class D (soft soil). To comply with EC8 - Part 5 (2004) requirements, the shear modulus of this soil has been reduced to 40% of its initial value in order to take into account the exhibition of non-linear soil deformations in soft soils for large levels of ground acceleration. The initial value of shear modulus has been computed using a shear wave velocity of 180m/sec and a soil density of 1900 kg/m³.

Table 3 Periods of the first two modes for structures A4a, A6a, A8a & B2a with and without SSI effects

Structure	1 st mode (sec)	2 nd mode (sec)
A4a - BRB FIX	1.26	0.82
A4a - BRB SSI	1.86	1.21
A6a - BRB FIX	1.92	1.25
A6a - BRB SSI	2.67	1.73
A8a - BRB FIX	2.21	1.45
A8a - BRB SSI	3.04	2.00
B2a - BRB FIX	0.30	0.24
B2a - BRB SSI	0.32	0.27

To get an idea of the influence of SSI on the vibrational behavior of the structures studied, Table 3 shows the periods corresponding to the first two modes of structures A4a, A6a, A8a & B2a for both fixed-base and with SSI effects included cases.

5. Seismic response analyses results

Due to the symmetry of the structures examined, the seismic response results of this section involve only the unfavorable structural responses, i.e., they correspond to the sides where two columns are oriented to provide minimum lateral stiffness. Interchangeability of the two horizontal components of the accelerograms has been taken into account when these unfavorable cases were sought. It was found that in the presence of SSI, the occurrence of localized storey mechanisms in lower storeys was not effectively controlled by the design and drift concentrations took place.

Mean IDR, RIDR and PFA estimates from the non-linear inelastic time-history analyses performed are presented in the following. In all analyses performed, the BRBs yielded first at small drift levels of about 0.5%. Even though beams and columns in BRB frames are designed to remain elastic, actual seismic demands may force yielding to occur in the surrounding frames outside of the BRB region. Therefore, mean seismic demands in terms of axial force and rotation in columns, of axial and shear forces and bending moment in BRB beams and of axial displacement in BRBs are also recorded. The effect of the configuration of the BRBs is also mentioned.

Due to space limitations, the seismic response and demands results presented and discussed in the following involve some of the structures of Table 1. Similar results in a qualitative sense have been found for the rest of the structures of Table 1 that are not presented herein. The presentation is performed by means of figures and tables that involve for comparison purposes both the fixed-base and with SSI effects included cases. Results for only the fixed-base case are shown when the effect of BRB configuration is discussed.

5.1 Peak interstorey drift ratios

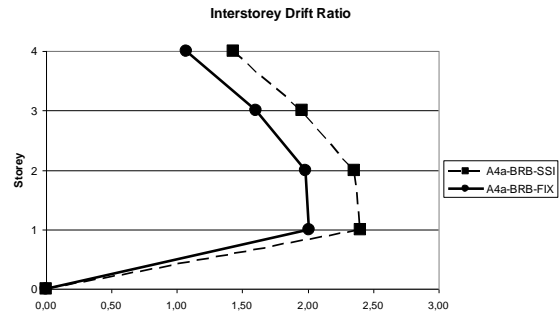


Fig. 9 Mean peak interstorey drift ratios for structure A4a

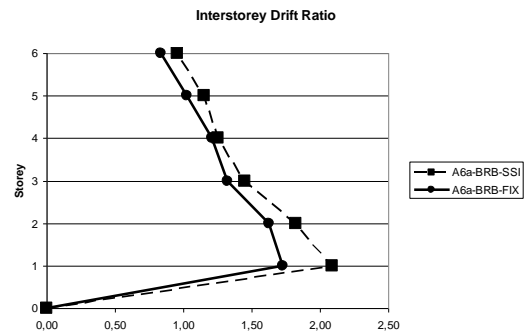


Fig. 10 Mean peak interstorey drift ratios for structure A6a

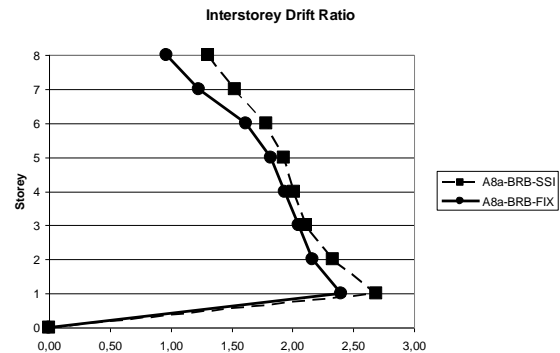


Fig. 11 Mean peak interstorey drift ratios for structure A8a

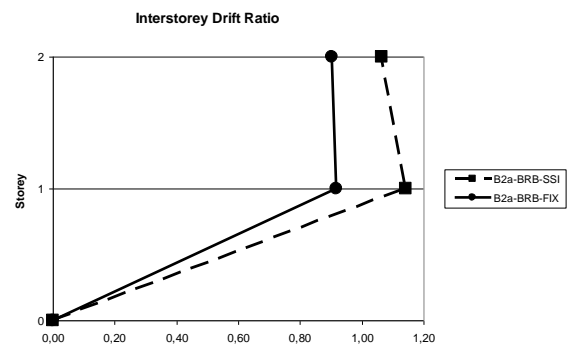


Fig. 12 Mean peak interstorey drift ratios for structure B2a

Figs. 9-11 display peak values of IDR for the case of structures A4a, A6a and A8a when subjected to the accelerograms of Table 2. From Figs. 9-11, it can be

concluded that large peak IDRs up to about 2.7% may be exhibited, surpassing, thus, the design value of 2.0%. Thus, it has been demonstrated that peak IDR values can be higher than those anticipated, increasing the probability of large values of permanent interstorey drift.

For structures A4a, A6a and A8a the peak drift values at all storeys became larger when SSI effects are taken into account in comparison to the fixed-base case. Smaller peak IDR values than the design value of 2.0% have been found for the structure B2a and are shown in Fig. 12.

5.2 Peak residual drift ratios

Figs. 13-15 display peak values of RIDR for the case of structures A4a, A6a and A8a when subjected to the accelerograms of Table 2. From these figures, it can be concluded that when SSI is taken into account peak RIDRs in the range of 0.53-0.85% may be exhibited, surpassing, thus, the threshold value of 0.5%. This means that significant structural damage is expected and the structure is practically non usable.

More specifically, peak residual drift values at all storeys for the structure A6a became larger than those of the fixed-base case. On the other hand, for structures A4a and A8a there is a small reduction in the peak residual drift values of storeys 1-2 and 4-8, respectively, when SSI is considered. It should be also noted that at least six from the seven accelerograms of Table 2 gave a RIDR value greater

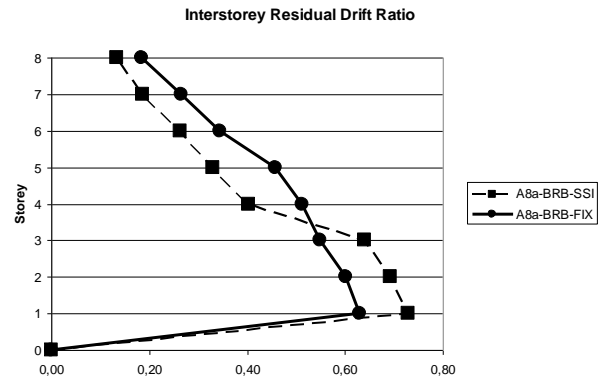


Fig. 15 Mean residual interstorey drift ratios for structure A8a

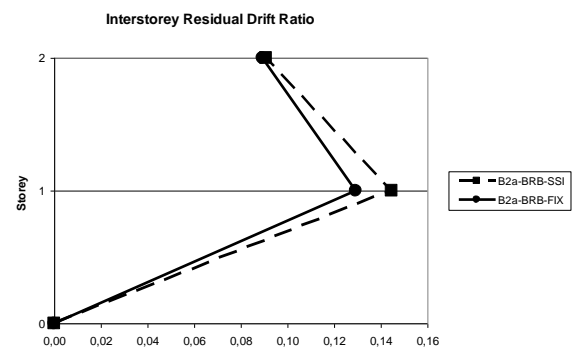


Fig. 16 Mean residual interstorey drift ratios for structure B2a

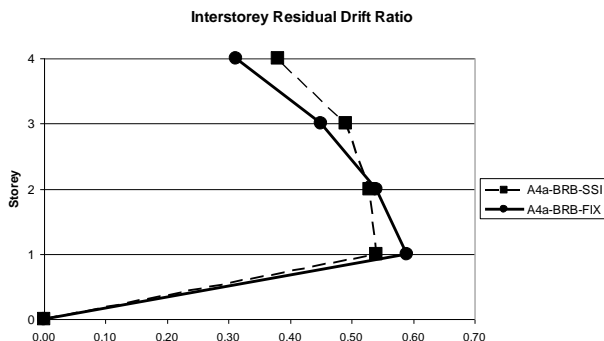


Fig. 13 Mean residual interstorey drift ratios for structure A4a

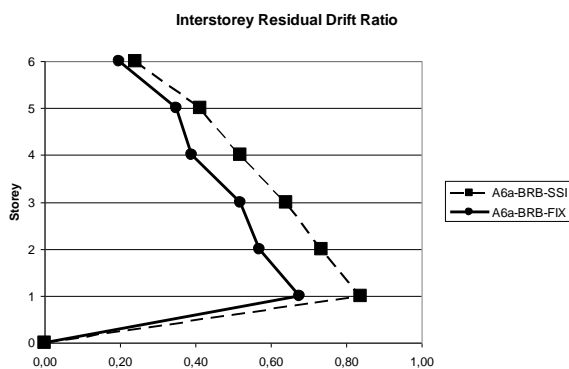


Fig. 14 Mean residual interstorey drift ratios for structure A6a

than 0.5% in all cases of structures of Type A examined. Significantly reduced RIDR values, due to the previously shown IDR values, have been found for the structure B2a, as shown in Fig. 16.

5.3 Peak floor accelerations

The range of PGA for the strongest component of the accelerograms of Table 2 is 0.37 g-0.70 g. In view of that, the ratio of PFA to PGA along height is shown in Figs. 17-20 for the case of structures A4a, A6a, A8a and B2a, respectively, when subjected to the accelerograms of Table 2. From Figs. 17-20, it can be concluded that when SSI is taken into account PFA/PGA values in the range of 0.5-1.7 g may be exhibited but the damage potential to non-structural elements should also involve the corresponding floor spectra.

Nevertheless, on the basis of Figs. 17-20, SSI effects may lead to increased (structures A4a, A8a, B2a) or reduced (structure A6a) values for the ratio PFA/PGA. Less than unity values for PFA/PGA means that the BRBs can limit the accelerations imparted to structure. However, significant amplifications of floor accelerations may also occur. In general, mean values of the ratio PFA/PGA, as those shown in Figs. 17-20 were not so sensitive to individual PFA/PGA values imposed from each accelerogram and do not reveal an unexpected or a problematic trend.

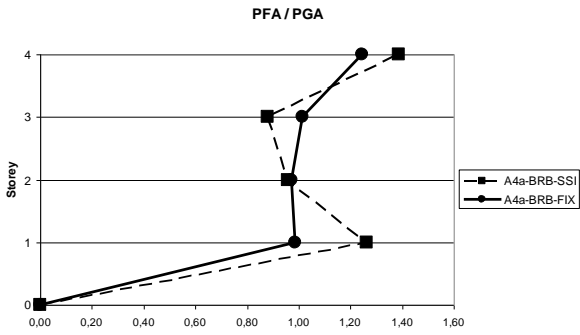


Fig. 17 Mean PFA/PGA values for structure A4a

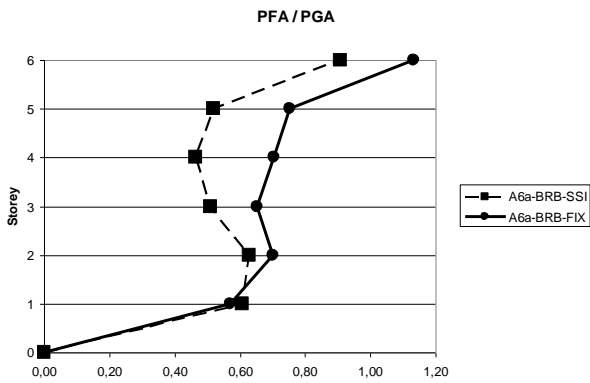


Fig. 18 Mean PFA/PGA values for structure A6a

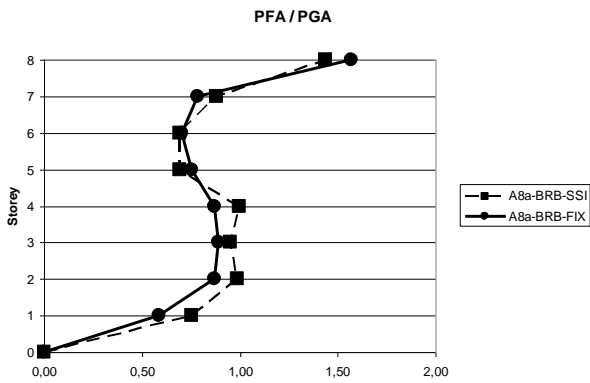


Fig. 19 Mean PFA/PGA values for structure A8a

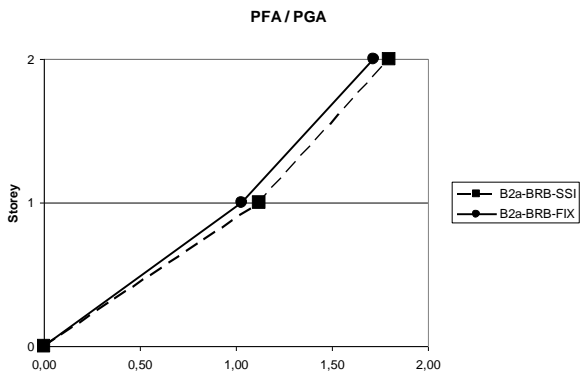


Fig. 20 Mean PFA/PGA values for structure B2a

5.4 Axial force and rotational demands in columns

Seismic demands in columns strongly depend on the extent and pattern of yielding that occur during the earthquake (Richards 2009). Considering the most heavily stressed column for structures A4a, A6a, A8a and B2a, figures 21-24 display the height wise ratio of the axial force to the design axial strength against flexural buckling. It can be concluded that for the fixed-base structures, the axial force of the lowest storey computed from the non-linear inelastic time-history analyses can reach to about 65% of the design value, thus, indicating the positive contribution of the BRBs. This contribution is even more pronounced when SSI effects are taken into account where the aforementioned ratio drops to about 35%.

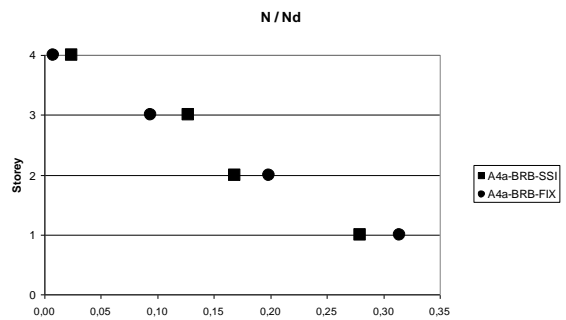


Fig. 21 Mean column axial force demands for structure A4a

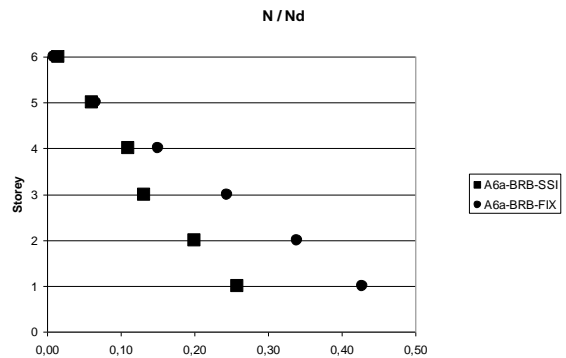


Fig. 22 Mean column axial force demands for structure A6a

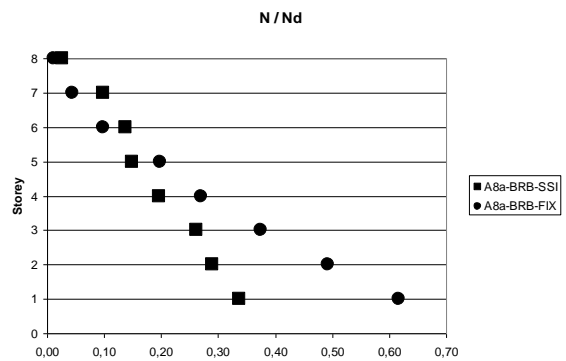


Fig. 23 Mean column axial force demands for structure A8a

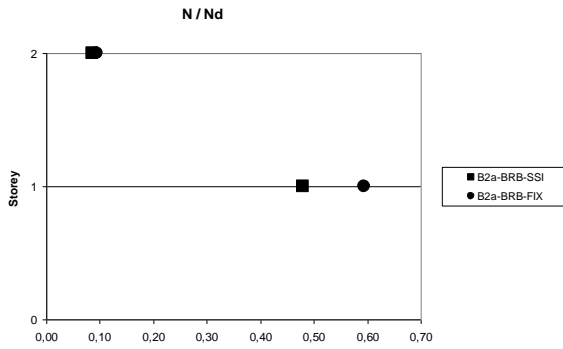


Fig. 24 Mean column axial force demands for structure B2a

At this point, it should be also mentioned that for the upper storeys, as shown in Figs. 21-23, SSI effects may lead to increased values of this ratio in comparison to the fixed-base case. In general, the computed axial force demands in conjunction with the computed inelastic rotational demands of about 0.07 rad (maximum value found) indicate that global failure of columns did not occur. This result is also consistent with the results of Newell and Uang (2008).

5.5 Demands in BRB beams and axial displacement of BRBs

Considering the BRB beams to be adequately braced, so that lateral torsional buckling is prevented, Table 4 presents their seismic demands in terms of axial and shear forces and bending moment for the cases of structures A4a, A6a and A8a. These force and moment demands have been normalized by the corresponding design strengths. From these results, it can be concluded that the BRB beam may fail due to flexure, whereas insignificant axial force and low shear force demands occur.

Mean values for the axial displacement of the BRB are presented in Table 5 for structures A4a, A6a and A8a. The design value of 0.084m (two times the design storey drift) was not exceeded, indicating that the BRB does not fail. The axial displacement of the BRB were found to be larger when SSI effects are taken into account.

Table 4 Mean demand ratio for BRB beams

Demand ratio	BRB - FIX			BRB - SSI		
	A4a	A6a	A8a	A4a	A6a	A8a
Axial	0.020	0.020	0.014	0.032	0.020	0.082
Shear	0.196	0.215	0.247	0.208	0.237	0.267
Moment	0.947	0.971	0.968	1.003	1.072	1.055

Table 5 Mean axial displacement values for the BRB

	BRB - FIX (m)	BRB - SSI (m)
A4a	0.028	0.042
A6a	0.034	0.052
A8a	0.041	0.054

5.6 Effect of the configuration of the BRBs

To study the effect of different BRB configurations, the fixed-base 6-storey structure has been analyzed employing the configurations of inverted V, diagonal bracing and multistory X-bracing, shown in Fig. 3. Peak response results in terms of IDR, RIDR and PFA/PGA are shown in Figs. 25-27, respectively. From these Figures, it can be concluded that the inverted V configuration leads to lower peak IDR and RIDR values and to larger peak PFA/PGA in comparison to the other two configurations. Even not shown herein due to space limitations, axial force demands in columns are slightly increased for the diagonal and multistory X-bracing configuration cases, without, however, the occurrence of a complete column failure. Moreover, axial displacement demands in BRBs are about the same, irrespectively of the configuration, and the BRB beam did not exhibit failure in flexure for the case of diagonal and multistory X-bracing configurations.

Similar results in a qualitative sense are obtained when SSI effects are considered. Nevertheless, the aforementioned conclusions regarding the configuration of the BRBs cannot be generalized and should be viewed only as representatives of the steel buildings studied herein. Mixed conclusions are expected if variations in connections of the BRBs within the frame are performed.

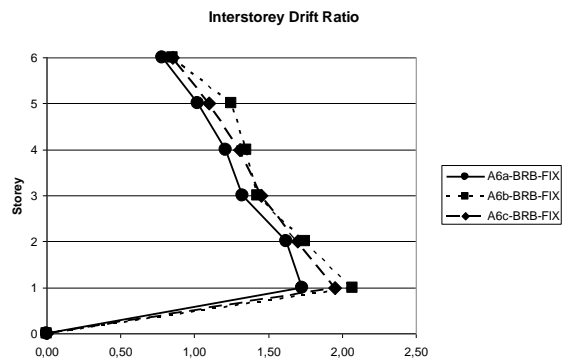


Fig. 25 Mean peak interstorey drift ratios for structure A6 and three BRB configurations

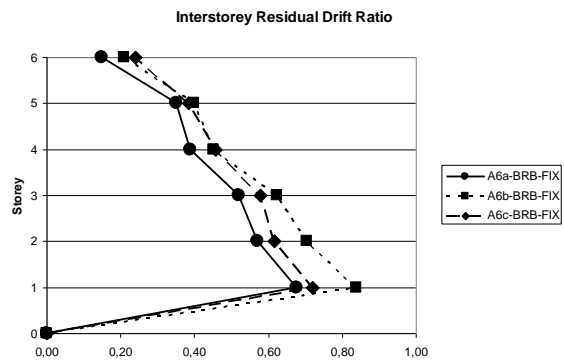


Fig. 26 Mean residual interstorey drift ratios for structure A6 and three BRB configurations

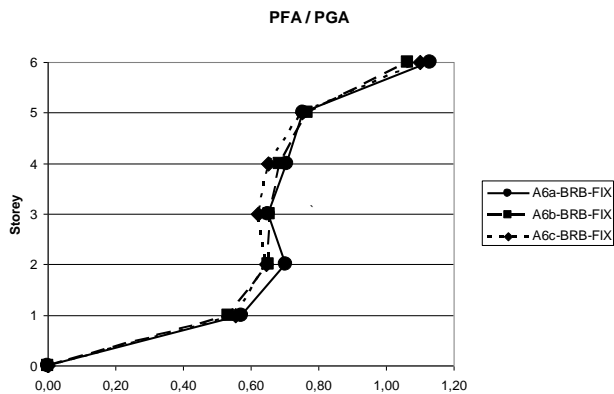


Fig. 27 Mean PFA/PGA values for structure A6 and three BRB configurations

6. Conclusions

The seismic response of some steel buckling-restrained braced structures including soil-structure interaction (SSI) effects has been studied by using three-dimensional non-linear inelastic time-history analyses employing accelerograms of recorded near-field ground motions. These structures have been designed for the highest seismic loads requirements holding for Greece.

From the results of these analyses it has been found that larger RIDRs at several storeys may occur when SSI effects are taken into account than when neglected. This is a direct result of the increased IDR values found that were well above the design IDR level. These IDR values have been exhibited, as expected, in lower storeys, due to increased deformational demands in view of the uniform distribution of the BRBs considered. On the other hand, PFA values did not reveal unexpected or problematic trends in the presence of SSI.

Finally, the large drifts due to SSI did not cause failure of columns and of BRBs. However, the BRB beam in an inverted V configuration may fail due to flexure.

References

- AISC (2010), *Seismic provisions for structural steel buildings*, American Institute of Steel Construction, Chicago, Illinois.
- Androić, B., Džeba, I. and Dujmović, D. (2000), *International structural steel sections*, Ernst & Sohn, Berlin, Germany.
- Ariyaratana, C. and Fahnestock, L.A. (2011), "Evaluation of buckling-restrained braced frame seismic performance considering reserve strength", *Eng. Struct.*, **33**(1), 77-89.
- Berman, J.W. and Bruneau, M. (2009), "Cyclic testing of a buckling restrained braced frame with unconstrained gusset connections", *J. Struct. Eng.*, ASCE, **135**(12), 1499-1510.
- Bosco, M. and Marino, E.M. (2013), "Design method and behavior factor for steel frames with buckling restrained braces", *Earthq. Eng. Struct. D.*, **42**(8), 1243-1263.
- Bruneau, M., Uang, C.M. and Sabelli, R. (2011), *Ductile design of steel structures*, McGraw Hill, New York, USA.
- Carr, A.J. (2004), *RUAUMOKO 3D - Inelastic dynamic analysis program: User's manual*, University of Canterbury, Christchurch, New Zealand.
- EC3 (2009), *Eurocode 3 - Design of steel structures, Part 1-1: General rules and rules for buildings*, European Committee for Standardization (CEN), Brussels.
- EC8 (2004), *Eurocode 8 - Design of structures for earthquake resistance, Part 5: Foundations, retaining structures and geotechnical aspects*, European Committee for Standardization (CEN), Brussels.
- EC8 (2009), *Eurocode 8 - Design of structures for earthquake resistance, Part 1: General rules, seismic actions and rules for buildings*, European Committee for Standardization (CEN), Brussels.
- Erochko, J., Christopoulos, C., Tremblay, R. and Choi, H. (2011), "Residual drift response of SMRFs and BRB frames in steel buildings designed according to ASCE 7-05", *J. Struct. Eng.*, ASCE, **137**(5), 589-599.
- Fahnestock, L.A., Ricles, J.M. and Sause, R. (2007), "Experimental evaluation of large-scale buckling-restrained braced frame", *J. Struct. Eng.*, ASCE, **133**(9), 1205-1214.
- Karavasilis, T.L., Kerawala, S. and Hale, E. (2012), "Hysteretic model for steel energy dissipation devices and evaluation of a minimal-damage seismic design approach for steel buildings", *J. Constr. Steel Res.*, **70**, 358-367.
- Kiggins, S. and Uang, C.M. (2006), "Reducing residual drift of buckling-restrained braced frames as a dual system", *Eng. Struct.*, **28**(11), 1525-1532.
- Lin, P.C., Tsai, K.C., Wu, A.C. and Chuang, M.C. (2014), "Seismic design and test of gusset connections for buckling-restrained braced frames", *Earthq. Eng. Struct. D.*, **43**(4), 565-587.
- McManus, P.S., Macmahon, A. and Puckett, J.A. (2013), "Buckling restrained braced frame with all-bolted gusset connections", *Eng. J.*, AISC, **50**(2), 89-116.
- Mulliken, J.S. and Karabalis, D.L. (1998), "Discrete model for dynamic through-the-soil coupling of 3-d foundations and structures", *Earthq. Eng. Struct. D.*, **27**(7), 687-710.
- Newell, J.D. and Uang, C.M. (2008), "Cyclic behavior of steel wide-flange columns subjected to large drift", *J. Struct. Eng.*, ASCE, **134**(8), 1334-1342.
- Palmer, K.D., Christopoulos, A.S., Lehman, D.E. and Roeder, C.W. (2014), "Experimental evaluation of cyclically loaded, large-scale, planar and 3-d buckling-restrained braced frames", *J. Constr. Steel Res.*, **101**, 415-425.
- Richards, P.W. (2009), "Seismic column demands in ductile braced frames", *J. Struct. Eng.*, ASCE, **135**(1), 33-41.
- Richards, P.W. and Miller, D.J. (2014), "High-yield-drift steel moment frames", *Proceedings of the 10th U.S. National Conference on Earthquake Engineering*, Anchorage, Alaska.
- Roy, J., Tremblay, R. and Léger, P. (2015), "Torsional effects in symmetrical steel buckling restrained braced frames: evaluation of seismic design provisions", *Earthq. Struct.*, **8**(2), 423-442.
- Sabelli, R., Mahin, S. and Chang, C. (2003), "Seismic demands on steel braced frame buildings with buckling-restrained braces", *Eng. Struct.*, **25**(5), 655-666.
- Sahoo, D.R. and Chao, S.H. (2015), "Stiffness-based design for mitigation of residual displacements of buckling-restrained braced frames", *J. Struct. Eng.*, ASCE, **141**(11), 04014229-1-04014229-13.
- Saxey, B. and Daniels, M. (2014), "Characterization of overstrength factors for buckling restrained braces", *Proceedings of the Australasian Structural Engineering Conference*, Auckland, New Zealand.
- SEAOC (2009), *Seismic design recommendations*, Structural Engineers Association of California, Sacramento, California.
- Tsampras, G., Sause, R., Fleischman, R.B. and Restrepo, J.I. (2017), "Experimental study of deformable connection consisting of buckling-restrained brace and rubber bearings to connect floor system to lateral force resisting system", *Earthq.*

Eng. Struct. D., doi: 10.1002/eqe.2856/full.

Wigle, V.R. and Fahnestock, L.A. (2010), "Buckling-restrained braced frame connection performance", *J. Constr. Steel Res.*, **66**(1), 65-74.

Zona, A. and Dall'Asta, A. (2012), "Elastoplastic model for steel buckling-restrained braces", *J. Constr. Steel Res.*, **68**(1), 118-125.

CC